OPEN ACCESS
atmosphere
ISSN 2073-4433
www.mdpi.com/journal/atmosphere

Supplementary Information

Joint Application of Concentration and δ^{18}O to Investigate the Global Atmospheric CO Budget. *Atmosphere* 2015, *6*, 547-578.

Keyhong Park [1,2,*], Louisa K. Emmons [3], Zhihui Wang [1] and John E. Mak [1]

[1] Institute for Terrestrial and Planetary Atmospheres, School of Marine and Atmospheric Sciences, State University of New York at Stony Brook, Stony Brook, NY 11794, USA; E-Mails: zhihuiw@gmail.com (Z.W.); john.mak@stonybrook.edu (J.E.M.)

[2] Division of Polar Ocean Environment, Korea Polar Research Institute, Incheon 406-840, South Korea

[3] Atmospheric Chemistry Division, National Center for Atmospheric Research, Boulder, CO 80301, USA; E-Mail: emmons@ucar.edu

* Author to whom correspondence should be addressed; E-Mail: keyhongpark@kopri.re.kr; Tel.: +82-32-760-5343; Fax: +82-32-760-5399.

Academic Editor: Robert W. Talbot

Supplementary. *A posteriori* modeled concentration and δ^{18}O

Since observed concentrations are expressed as (Equation 4), the relationship between the measured and optimized modeled concentrations can be expressed as:

$$\hat{y} = \mathbf{K}\hat{x} + \hat{e} \tag{A1}$$

where $\mathbf{K}\hat{x}$ the optimized concentrations ($\hat{y}$) and $\hat{e}$ is *a posteriori* error matrix.

Updating the modeled isotope ratios with the optimized source information is more complicated because isotope ratio (δ) is the 'relative' abundances of the two isotopologues. The implementation of the *a posteriori* isotopic source signatures to the optimization of modeled [C^{16}O] and [C^{18}O] is shown in below.

Modeled concentrations of isotopologues are expressed as:

$$a = \sum_j K_{a,j} x_{a,j}, \quad b = \sum_j K_{b,j} x_{b,j} \tag{A2}$$

where i is an index for major and minor isotope (a: major isotope, b: minor isotope) and j is an index for the sources. We assume two sources for simplification.

The abundance of major and minor isotope can linearly related by using isotopic source ratio (γ_j).

$$x_{a,j} = \gamma_j x_{b,j} \tag{A3}$$

The concentration of a and b can be rewritten in a matrix form:

$$\begin{pmatrix} \mathbf{a} \\ \mathbf{b} \end{pmatrix} = \begin{pmatrix} \mathbf{K}_{a,1} & \mathbf{K}_{a,2} \\ \mathbf{K}_{b,1}/\gamma_1 & \mathbf{K}_{b,2}/\gamma_2 \end{pmatrix} \begin{pmatrix} \mathbf{x}_{a,1} \\ \mathbf{x}_{a,2} \end{pmatrix}$$

$$= \begin{pmatrix} \mathbf{K}_{a,1}\mathbf{x}_{a,1} & \mathbf{K}_{a,2}\mathbf{x}_{a,2} \\ \mathbf{K}_{b,1}\mathbf{x}_{a,1}/\gamma_1 & \mathbf{K}_{b,2}\mathbf{x}_{a,2}/\gamma_2 \end{pmatrix} \begin{pmatrix} \mathbf{f}_1 \\ \mathbf{f}_2 \end{pmatrix} = \begin{pmatrix} \mathbf{a}_1^* & \mathbf{a}_2^* \\ \mathbf{b}_1^* & \mathbf{b}_2^* \end{pmatrix} \begin{pmatrix} \mathbf{f}_1 \\ \mathbf{f}_2 \end{pmatrix} \tag{A4}$$

$$\mathbf{f}_1 \text{ and } \mathbf{f}_2 : \text{a unit source strength factor}$$

where, $\mathbf{a}_1^*$, $\mathbf{a}_2^*$, $\mathbf{b}_1^*$, and $\mathbf{b}_2^*$ represent the modeled concentration.

The optimized f_j ($\hat{f}_j$) can be obtained by the inversion analysis. Then, *a posteriori a* can be expressed as:

$$\hat{a} = \sum_j K_{a,j}\hat{x}_{a,j} = \sum_j K_{a,j}x_{a,j}\hat{f}_j \tag{A5}$$

The *a posteriori* linear relation between the major and the minor isotopes is:

$$\hat{x}_{a,j} = \gamma_j^* \hat{x}_{b,j} \tag{A6}$$

Also, using the updated isotopic source ratio (γ_j^*), *a posteriori b* can be expressed as a function of *a priori* modeled concentration ($K_{b,j}x_{b,j}$).

$$\hat{b} = \sum_j K_{b,j}\hat{x}_{b,j} = \sum_j \frac{\gamma_j}{\gamma_j^*} K_{b,j}x_{b,j}\hat{f}_j, \quad \text{for fixed isotopic source signatures } \frac{\gamma_j}{\gamma_j^*} = 1 \tag{7}$$

If isotopic source signatures are well defined, γ_j/γ_j^* should be close to 1 and no further treatment for updating *a posteriori* source signature information is necessary. For the oxygen isotopes of CO, in comparison with the fixed isotopic source ratios, *a posteriori* $\delta^{18}O$ is closer to the observation with the updated isotopic source information (Section 5, Table S6). This implies the joint inversion analysis provides more useful results if *a posteriori* source information is applied along with the optimized source strengths when isotopic source signatures contain large error.

Table S1. Estimates of the global tropospheric CO budget (TgCO/year).

Sources	Duncan *et al.* [67]	*IPCC 2001*
Oxidation of CH_4	778–861	800
Oxidation of Isoprene	170–184	270
Oxidation of Terpene	68–71	~ 0
Oxidation of industrial NMHC	102–106	110
Oxidation of biomass NMHC	45–57	30
Oxidation of Methanol	95–103	-
Oxidation of Acetone	21	20
Vegetation	-	150
Oceans	-	50
Biomass burning	406–516	700
Fossil and domestic fuel	550–570	650
Total sources	2236–2489	2780
Sinks		
OH reaction		1500–2700

Table S2. Isotope Composition of CO sources.

Sources	$\delta^{18}O$, ‰	$\delta^{13}C$, ‰
Fossil fuel combustion	+23.5[a,b], +24[c], +22[d] +25.3[e] (gasoline) +15.1[e] (diesel)	−27.5[a]
Biomass Burning	+16.3[b], +18±1[c] +3~+18.4[f] (smoldering) +16.2 ~ +26.0[f] (flaming)	−21.3[i], −24.5[j]
Methane oxidation	0[b,d], +15[c]	−52.6[k]
NMHC oxidation	0[b,d], +14.9[c]	−32.2[c]
Biogenic	?[g]	?[g]
Oceans	+15[h]	−40[h]

[a] *Stevens et al.* [65]; [b] *Brenninkmeijer* [42]; [c] *Stevens and Wagner* [62]; [d] *Brenninkmeijer and Röckmann* [10]; [e] *Tsunogai et al.* [64]; [f] *Kato et al.* [83]; [g] *no data has been reported*; [h] *Nakagawa et al.* [66]; [i] *Conny et al.* [85]; [j] *Conny* [86]; [k] Values based on the $\delta^{13}C_{CH4}$ (−47.2 ‰ [*Quay et al.*, [87]], and the fractionation in CH_4 + OH (5.4 ‰).

Table S3. Data availability during the model simulation period (April 1996–December 2004).

Year	Month	model	SCO	BHD	ICE	ZEP	ALT	MLO	IZO	RPB
96	4	spin-								
	~	up								
96	10	o	o	o		o	o		o	o
	~	o	o	o		o	o		o	o
97	8	o	o	o		o	o		o	o
97	9	o		o		o	o		o	o
97	10	o				o	o		o	o
97	11	o	o			o	o		o	o
97	12	o	o	o		o	o		o	o
98	1	o	o	o		o	o		o	o
	~	o	o	o		o			o	o
98	10	o	o	o		o		o	o	o
	~	o	o	o		o		o	o	o
99	4	o	o	o		o		o	o	o
99	5	o	o	o		o		o		o
99	6	o	o	o		o		o		o
	~	o	o	o				o		o
99	12	o	o	o				o		o
	~	o		o				o		o
00	5	o		o				o		o
00	6	o		o				o		
00	7	o	o	o				o		
	~	o	o	o				o		
01	3	o	o	o				o		
	~	o	o	o						
01	12	o	o	o						

Table S3. *Cont.*

Year	Month	model	SCO	BHD	ICE	ZEP	ALT	MLO	IZO	RPB
02	1	o	o							
02	2	o	o							
02	3	o	o	o						
	~	o	o	o						
03	8	o	o	o				o		
	~	o	o	o				o		
04	1	o	o	o	o			o		
	~	o	o	o	o			o		
04	9	o	o	o	o			o		
04	10	o		o	o			o		
04	11	o		o	o			o		
04	12	o	o	o	o			o		

Table S4. Influence of emissions (FF, BF, BB) of each hemisphere at each station. For each source, the first two rows show the fraction of the SH emission of the source and the total concentration and the last two rows show the fraction of the NH's.

Station	ALT	ZEP	ICE	IZO	MLO	RPB	BHD	SCO
SH-[CO]ff/total-[CO]ff	0.3%	0.2%	0.2%	0.9%	1.9%	1.4%	66.0%	60.4%
SH-[CO]ff/total-[CO]	0.1%	0.1%	0.1%	0.2%	0.3%	0.2%	98.3%	98.3%
NH-[CO]ff/total-[CO]ff	99.7%	99.8%	99.8%	99.1%	98.1%	98.6%	34.0%	39.6%
NH-[CO]ff/total-[CO]	99.9%	99.9%	99.9%	99.8%	99.7%	99.8%	1.7%	1.7%
SH-[CO]bf/total-[CO]bf	1.6%	1.4%	1.6%	3.5%	3.9%	5.2%	47.3%	47.2%
SH-[CO]bf/total-[CO]	0.1%	0.1%	0.1%	0.4%	0.5%	0.5%	98.1%	98.0%
NH-[CO]bf/total-[CO]bf	98.4%	98.6%	98.4%	96.5%	96.1%	94.8%	52.7%	52.8%
NH-[CO]bf/total-[CO]	99.9%	99.9%	99.9%	99.6%	99.5%	99.5%	1.9%	2.0%
SH-[CO]bb/total-[CO]bb	8.1%	7.7%	8.9%	19.1%	21.3%	26.0%	83.7%	82.4%
SH-[CO]bb/total-[CO]	0.8%	0.8%	0.8%	1.9%	2.3%	2.9%	97.9%	97.7%
NH-[CO]bb/total-[CO]bb	91.9%	92.3%	91.1%	80.9%	78.7%	74.0%	16.3%	17.6%
NH-[CO]bb/total-[CO]	99.2%	99.2%	99.2%	98.1%	97.7%	97.1%	2.1%	2.3%

Table S5. Model-observation difference, correlation and chi-square of each station (forward model results).

Station	Latitude	Difference		Correlation		Chi-square	
		[CO]	$\delta^{18}O$	[CO]	$\delta^{18}O$	[CO]	$\delta^{18}O$
Alert	82° 27' N	14.973	1.034	0.933	0.978	0.391	0.129
Spitzbergen	78° 54' N	12.220	0.986	0.917	0.961	0.226	0.123
Iceland	63° 15' N	9.028	1.929	0.926	0.929	0.171	0.709
Izaña	28° 18' N	13.555	1.321	0.921	0.928	0.561	0.364
Mauna Loa	19° 32' N	12.017	4.832	0.694	0.656	0.730	5.109
Barbados	13° 10' N	18.140	4.621	0.721	0.704	1.655	4.576
Baring Head	41° 18' S	6.400	3.253	0.789	0.555	0.831	5.299
Scott Base	77° 51' S	6.195	2.491	0.843	0.728	0.606	1.976

Table S6. *A priori* (modeled) and *a posteriori* (optimized) model-observation difference (ppbv).

RPB		**1997**	**1998**	**2004**
[CO]	Observation			
	Modeled	15.35	27.60	
	Optimized ([CO] only)	8.93	17.46	
	Optimized (Joint Simultaneous)	8.40	17.45	
	Optimized (Joint Sequential)	8.54	17.42	
d18O	Observation			
	Modeled	3.71	4.88	
	Optimized (Joint Simultaneous)-adjusted isotopic source ratio	1.79	3.08	
	Optimized (Joint Sequential)-adjusted isotopic source ratio	2.02	4.52	
	Optimized (Joint Simultaneous)-fixed isotopic source ratio	2.33	5.41	
	Optimized (Joint Sequential)-fixed isotopic source ratio	2.27	5.32	
IZO		**1997**	**1998**	**2004**
[CO]	Observation			
	Modeled	10.39	17.85	
	Optimized ([CO] only)	8.85	4.86	
	Optimized (Joint Simultaneous)	9.03	4.71	
	Optimized (Joint Sequential)	9.09	4.69	
d18O	Observation			
	Modeled	1.73	1.18	
	Optimized (Joint Simultaneous)-adjusted isotopic source ratio	1.04	0.56	
	Optimized (Joint Sequential)-adjusted isotopic source ratio	1.11	0.94	
	Optimized (Joint Simultaneous)-fixed isotopic source ratio	1.29	1.79	
	Optimized (Joint Sequential)-fixed isotopic source ratio	1.30	1.70	
MLO		**1997**	**1998**	**2004**
[CO]	Observation			
	Modeled			12.72
	Optimized ([CO] only)			11.97
	Optimized (Joint Simultaneous)			11.67
	Optimized (Joint Sequential)			11.76
d18O	Observation			
	Modeled			4.90
	Optimized (Joint Simultaneous)-adjusted isotopic source ratio			2.52
	Optimized (Joint Sequential)-adjusted isotopic source ratio			4.00
	Optimized (Joint Simultaneous)-fixed isotopic source ratio			5.01
	Optimized (Joint Sequential)-fixed isotopic source ratio			4.96

Table S6. *Cont.*

ZEP		**1997**	**1998**	**2004**
[CO]	Observation			
	Modeled	15.65	13.53	
	Optimized ([CO] only)	9.17	8.11	
	Optimized (Joint Simultaneous)	8.86	7.26	
	Optimized (Joint Sequential)	8.60	6.78	
d18O	Observation			
	Modeled	0.76	1.24	
	Optimized (Joint Simultaneous)-adjusted isotopic source ratio	0.84	0.90	
	Optimized (Joint Sequential)-adjusted isotopic source ratio	1.74	0.70	
	Optimized (Joint Simultaneous)-fixed isotopic source ratio	1.43	0.97	
	Optimized (Joint Sequential)-fixed isotopic source ratio	1.46	0.94	
ALT		**1997**	**1998**	**2004**
[CO]	Observation			
	Modeled	16.91		
	Optimized ([CO] only)	7.87		
	Optimized (Joint Simultaneous)	7.83		
	Optimized (Joint Sequential)	8.01		
d18O	Observation			
	Modeled	1.47		
	Optimized (Joint Simultaneous)-adjusted isotopic source ratio	0.78		
	Optimized (Joint Sequential)-adjusted isotopic source ratio	0.75		
	Optimized (Joint Simultaneous)-fixed isotopic source ratio	1.14		
	Optimized (Joint Sequential)-fixed isotopic source ratio	1.14		
ICE		**1997**	**1998**	**2004**
[CO]	Observation			
	Modeled			9.74
	Optimized ([CO] only)			8.27
	Optimized (Joint Simultaneous)			7.72
	Optimized (Joint Sequential)			7.51
d18O	Observation			
	Modeled			1.94
	Optimized (Joint Simultaneous)-adjusted isotopic source ratio			0.92
	Optimized (Joint Sequential)-adjusted isotopic source ratio			1.52
	Optimized (Joint Simultaneous)-fixed isotopic source ratio			2.41
	Optimized (Joint Sequential)-fixed isotopic source ratio			2.35

Table S6. *Cont.*

BHD		**1997**	**1998**	**2004**
[CO]	Observation			
	Modeled	9.71	5.83	9.54
	Optimized ([CO] only)	4.84	4.00	3.06
	Optimized (Joint Simultaneous)	4.92	4.01	3.09
	Optimized (Joint Sequential)	4.88	4.23	3.17
d18O	Observation			
	Modeled	4.93	3.53	2.48
	Optimized (Joint Simultaneous)-adjusted isotopic source ratio	1.34	0.86	0.63
	Optimized (Joint Sequential)-adjusted isotopic source ratio	3.04	1.92	0.63
	Optimized (Joint Simultaneous)-fixed isotopic source ratio	4.50	3.65	1.90
	Optimized (Joint Sequential)-fixed isotopic source ratio	4.50	3.60	1.94
SCO		**1997**	**1998**	**2004**
[CO]	Observation			
	Modeled	5.34	5.66	7.74
	Optimized ([CO] only)	2.76	2.60	1.74
	Optimized (Joint Simultaneous)	2.71	2.58	1.70
	Optimized (Joint Sequential)	2.99	2.49	1.78
d18O	Observation			
	Modeled	3.38	3.18	1.63
	Optimized (Joint Simultaneous)-adjusted isotopic source ratio	0.93	0.82	0.43
	Optimized (Joint Sequential)-adjusted isotopic source ratio	1.53	1.85	0.42
	Optimized (Joint Simultaneous)-fixed isotopic source ratio	2.91	3.31	1.15
	Optimized (Joint Sequential)-fixed isotopic source ratio	2.90	3.26	1.17

Table S7. *A priori* and *a posteriori* oxygen isotope source signatures of CO. The *a posteriori* values are obtained from the standard inversion run of this study (simultaneous inversion).

	Fossil	**Biomass**	**CH4**	**NMHC**	**Biofuel**	**Ocean**	**Biogenic**
97NH	21.5	18.2	2.9	1.3	14.7	18.2	−0.4
98NH	21.5	14.1	2.4	5.0	22.5	17.5	−1.5
04NH	21.5	12.5	2.5	5.0	15.4	16.0	5.0
97SH	23.5	12.5	3.0	5.0	18.1	20.0	5.0
98SH	23.8	12.5	2.2	5.0	18.5	19.2	4.5
04SH	23.2	12.5	0.9	5.0	16.2	17.7	2.7
a priori	23.5	17.5	0.0	0.0	17.5	15.0	0.0

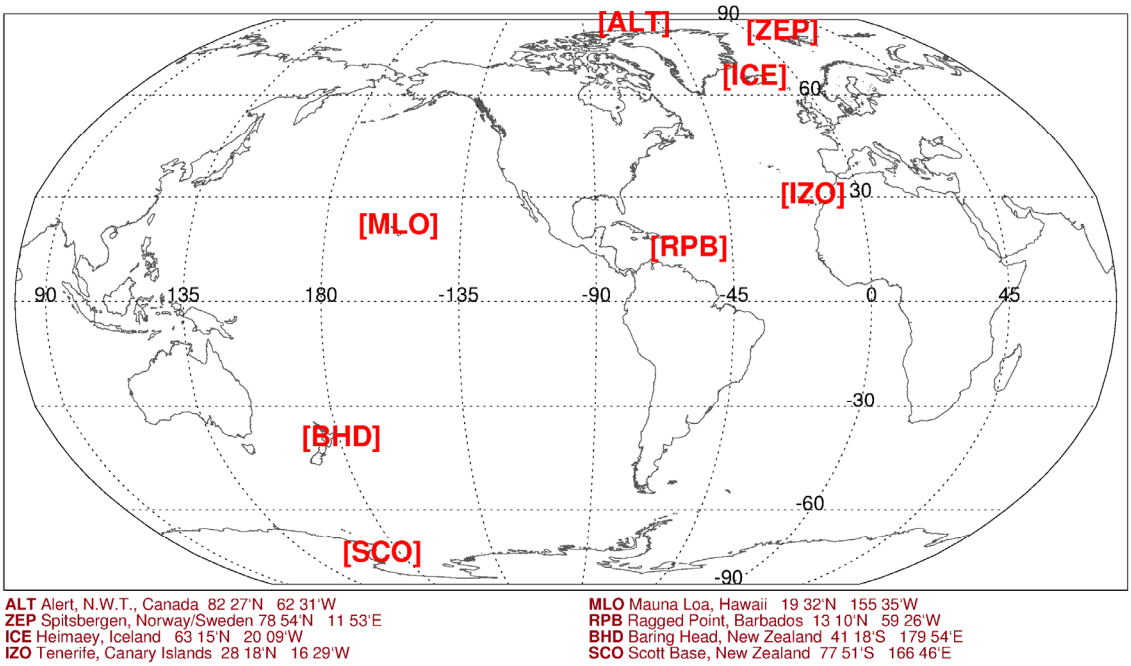

Figure S1. Measurement stations for [CO] and isotope ratios. Alert, Canada (ALT), Spitsbergen, Norway (ZEP), and Izana, Canary Islands (IZO) are measured by Max Plank Institute for chemistry, Germany [27,88], Baring Head, New Zealand (BHD) and Scott Base, Antarctica (SCO) are measured by National Institute for Water and Atmospheric Research, New Zealand [42,89], and Mauna Loa, USA (MLO), Ragged Point, Barbados (RPB), and Heimaey, Iceland (ICE) are measured by Stony Brook University [36].

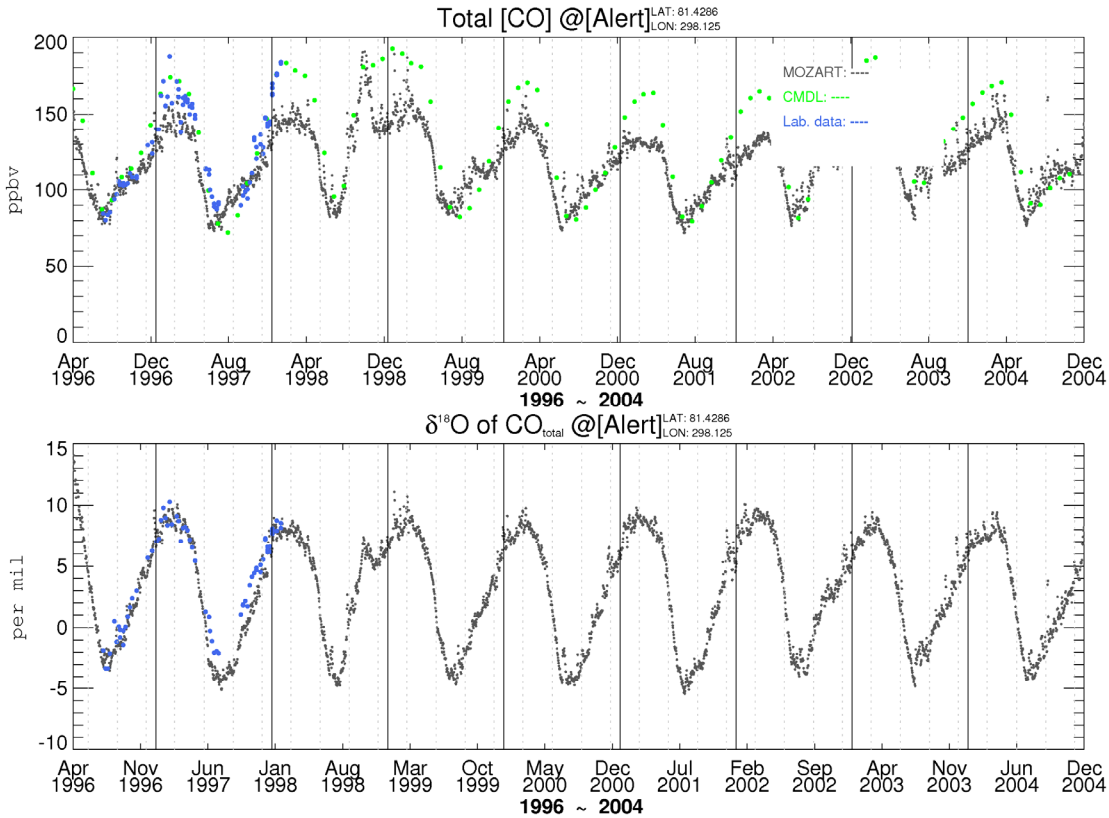

Figure S2. *Cont.*

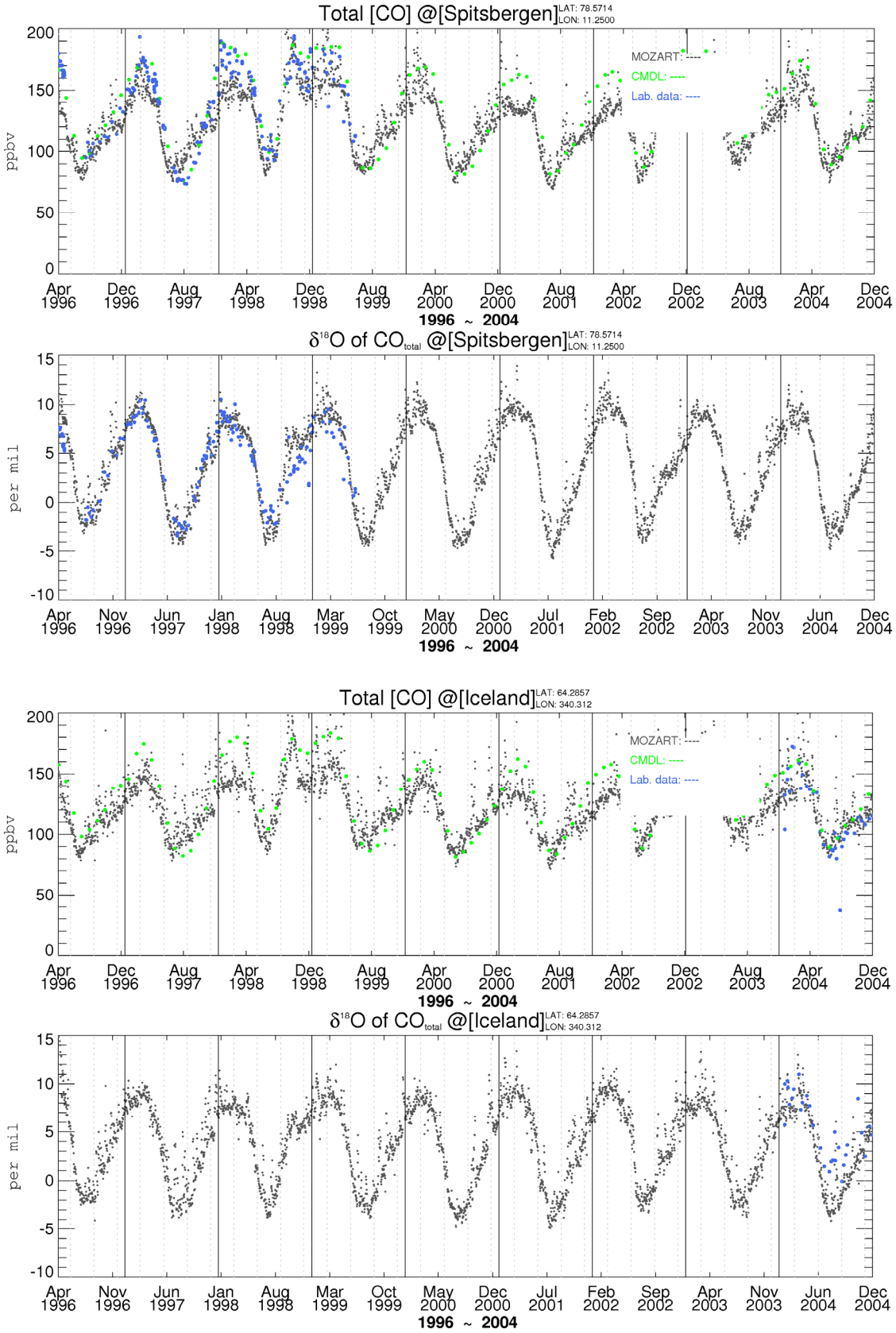

Figure S2. *Cont.*

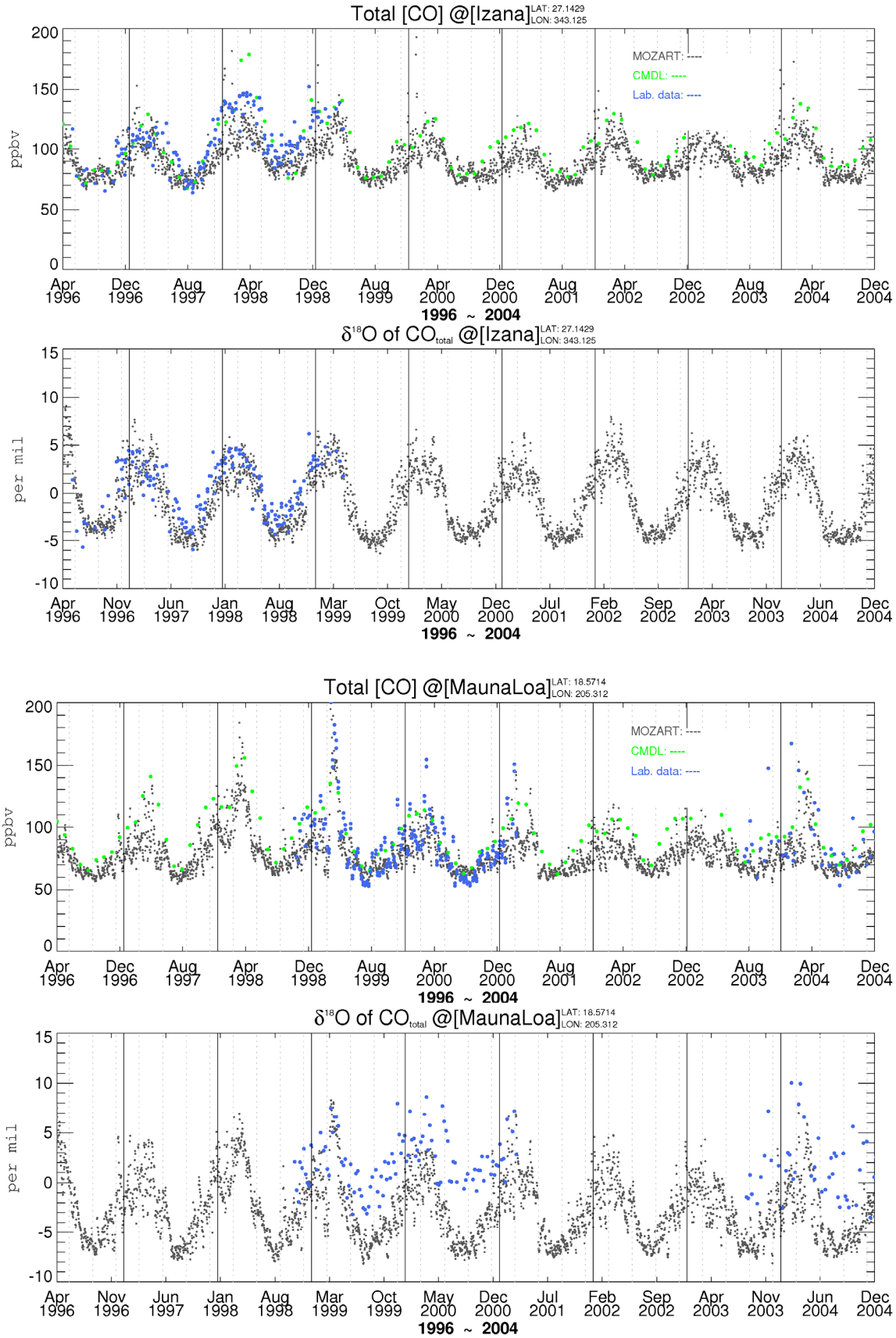

Figure S2. *Cont.*

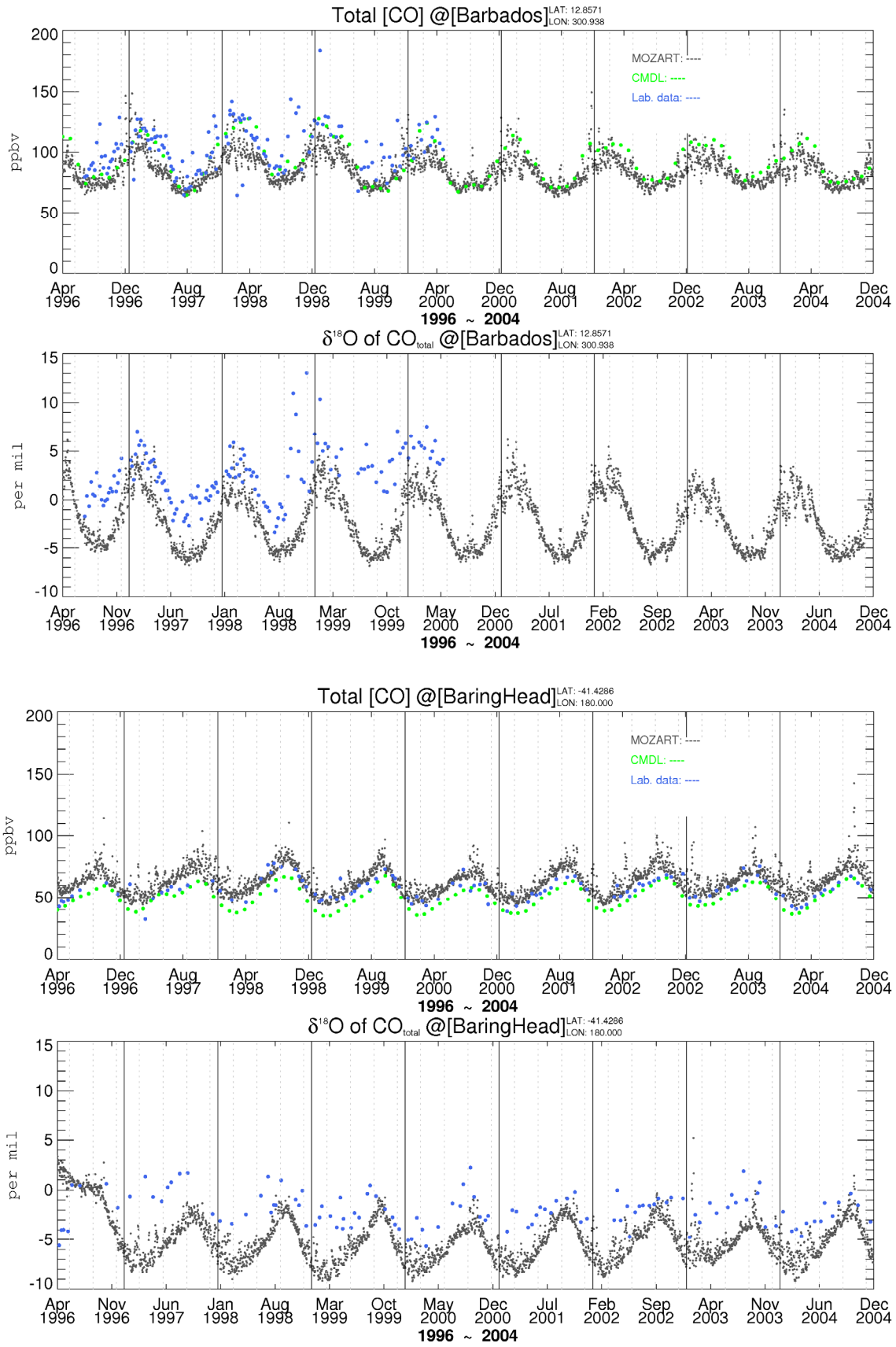

Figure S2. *Cont.*

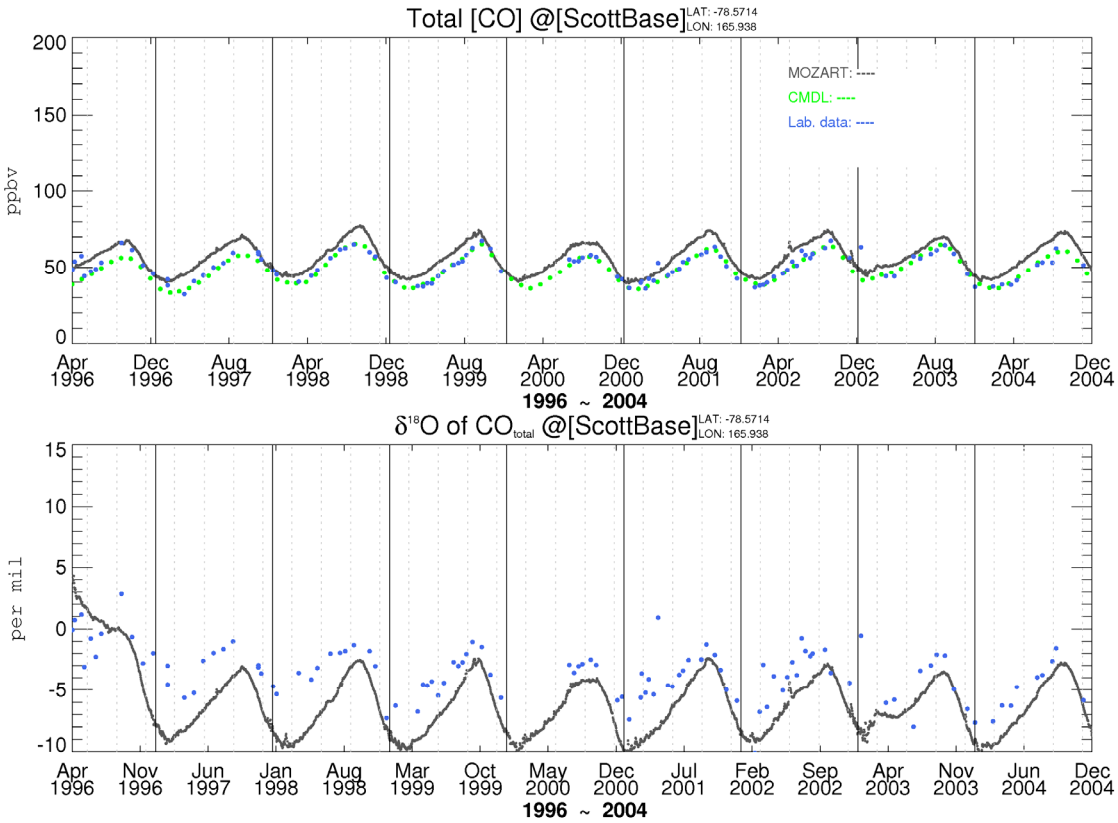

Figure S2. MOZART-4 simulation results; the gray dots are modeled [CO] and $\delta^{18}O$, the green dots are NOAA [CO] and the blue dots are [CO] and $\delta^{18}O$ used in this study.

Alert

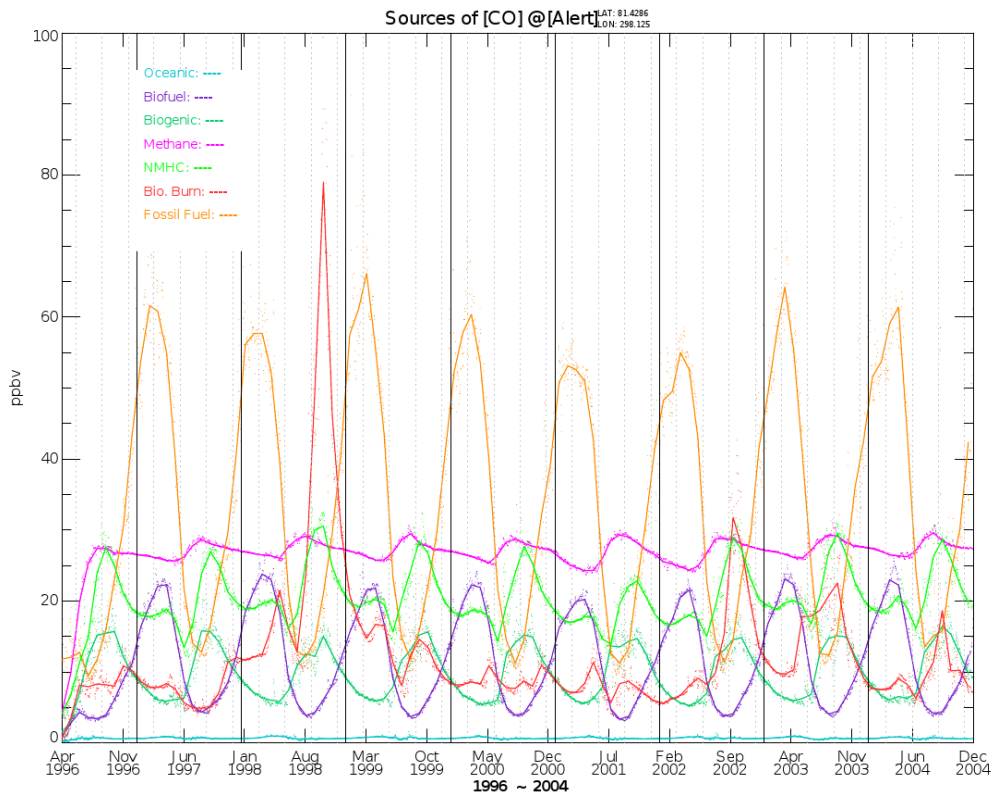

Figure S3. *Cont.*

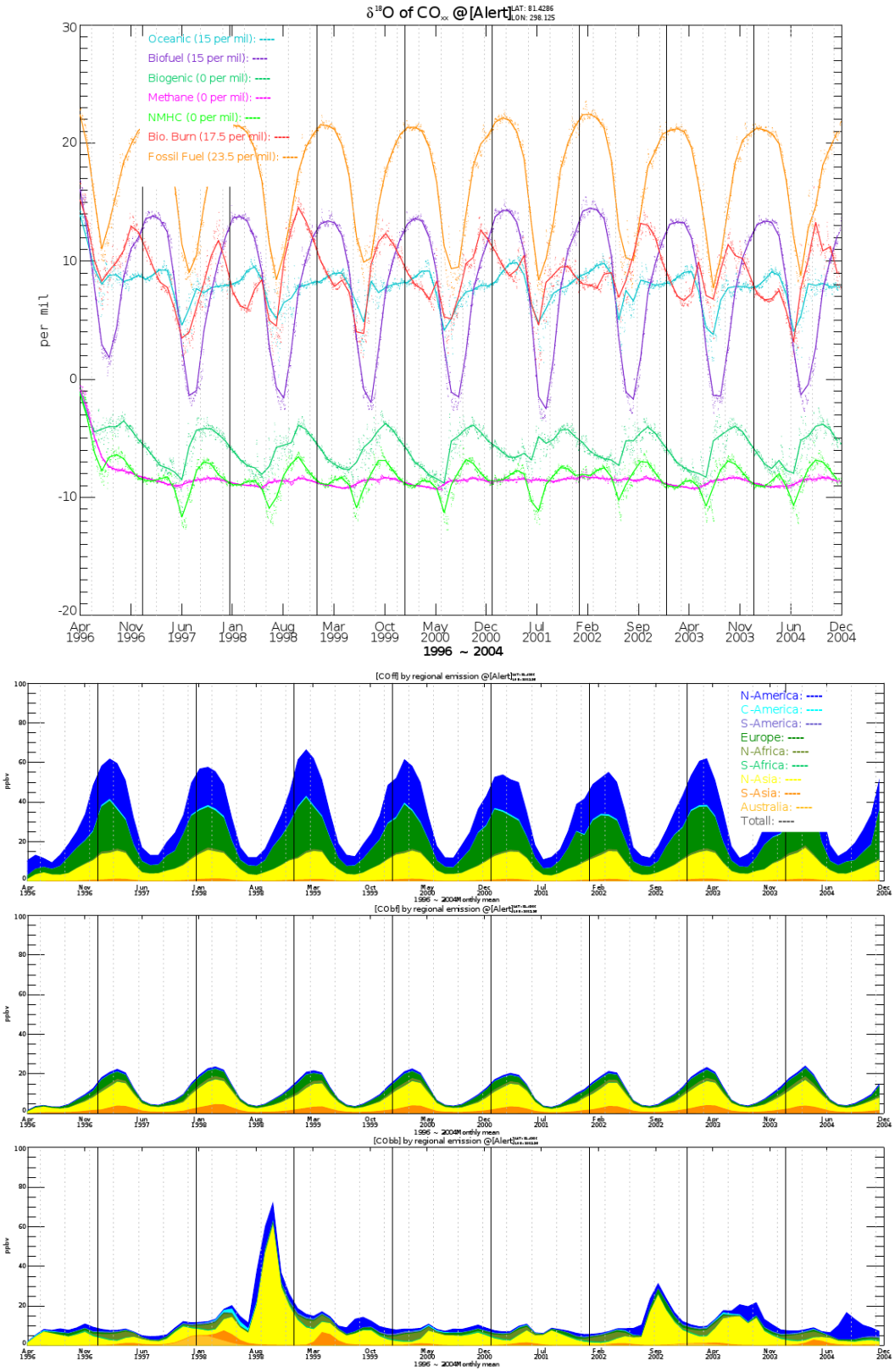

Figure S3. *Cont.*

Spitzbergen

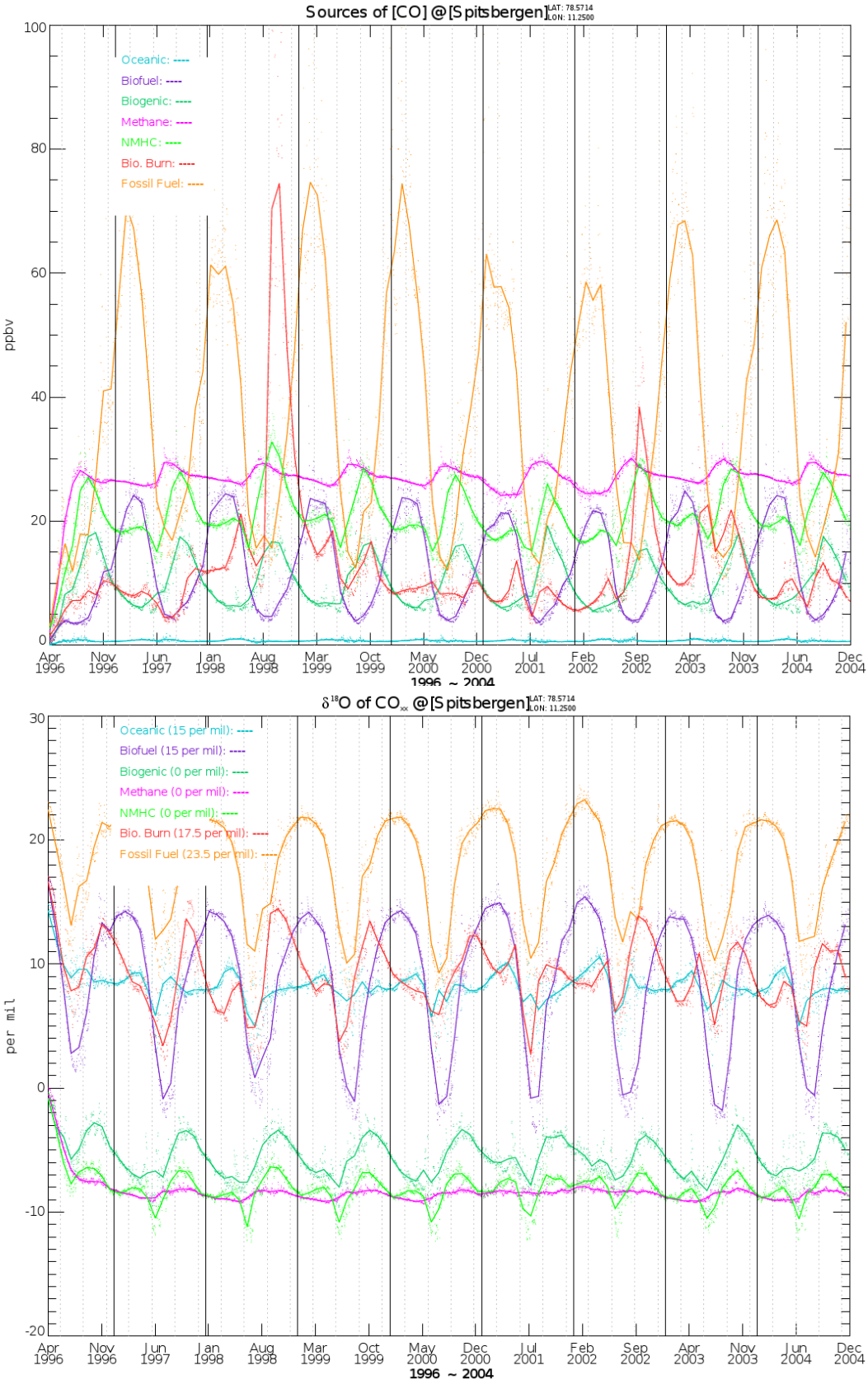

Figure S3. *Cont.*

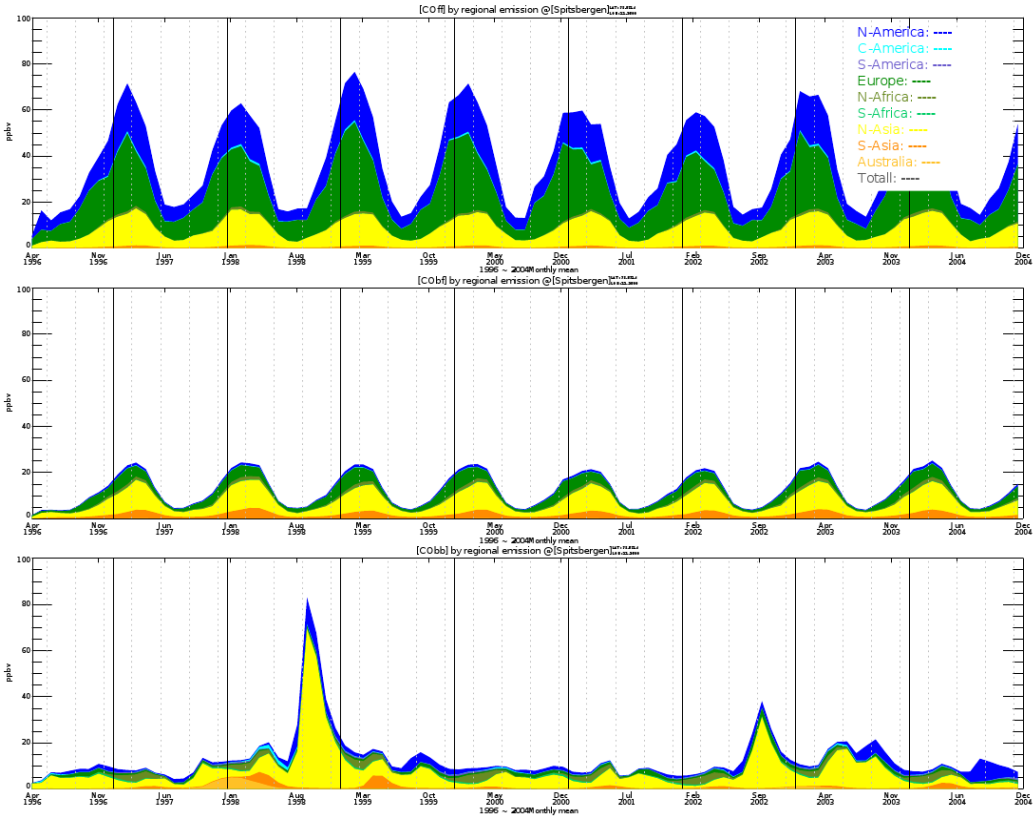

Iceland

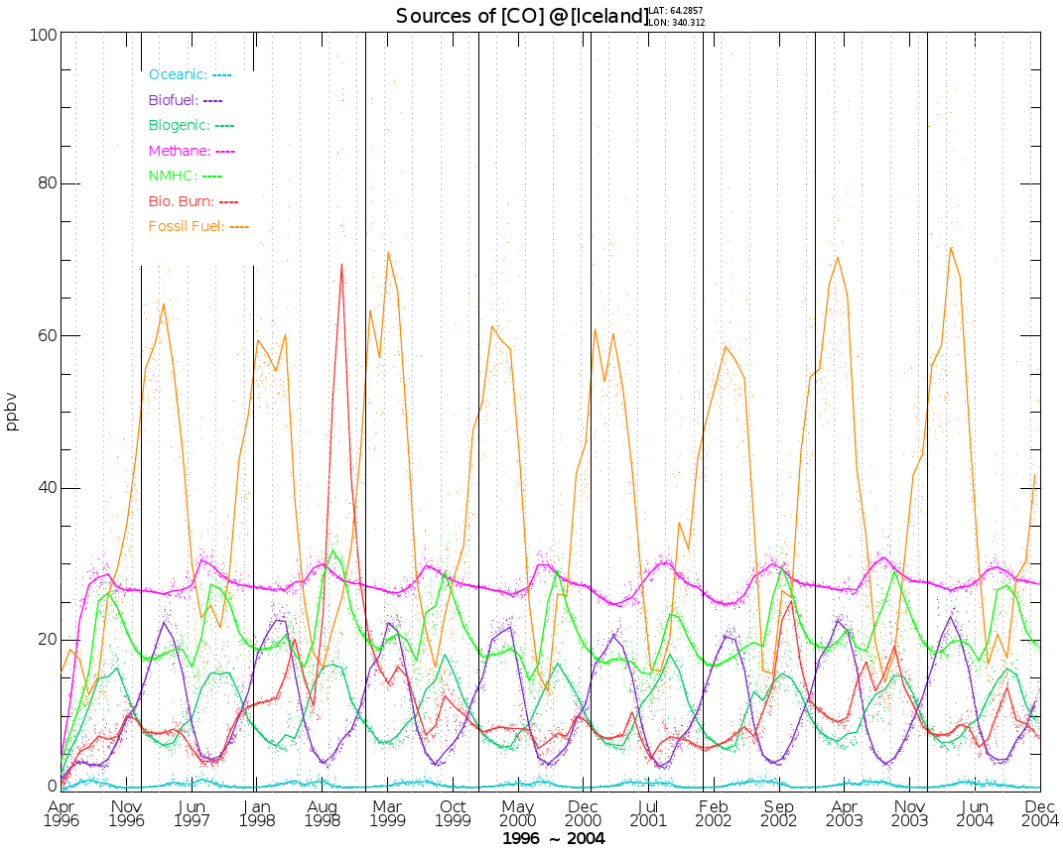

Figure S3. *Cont.*

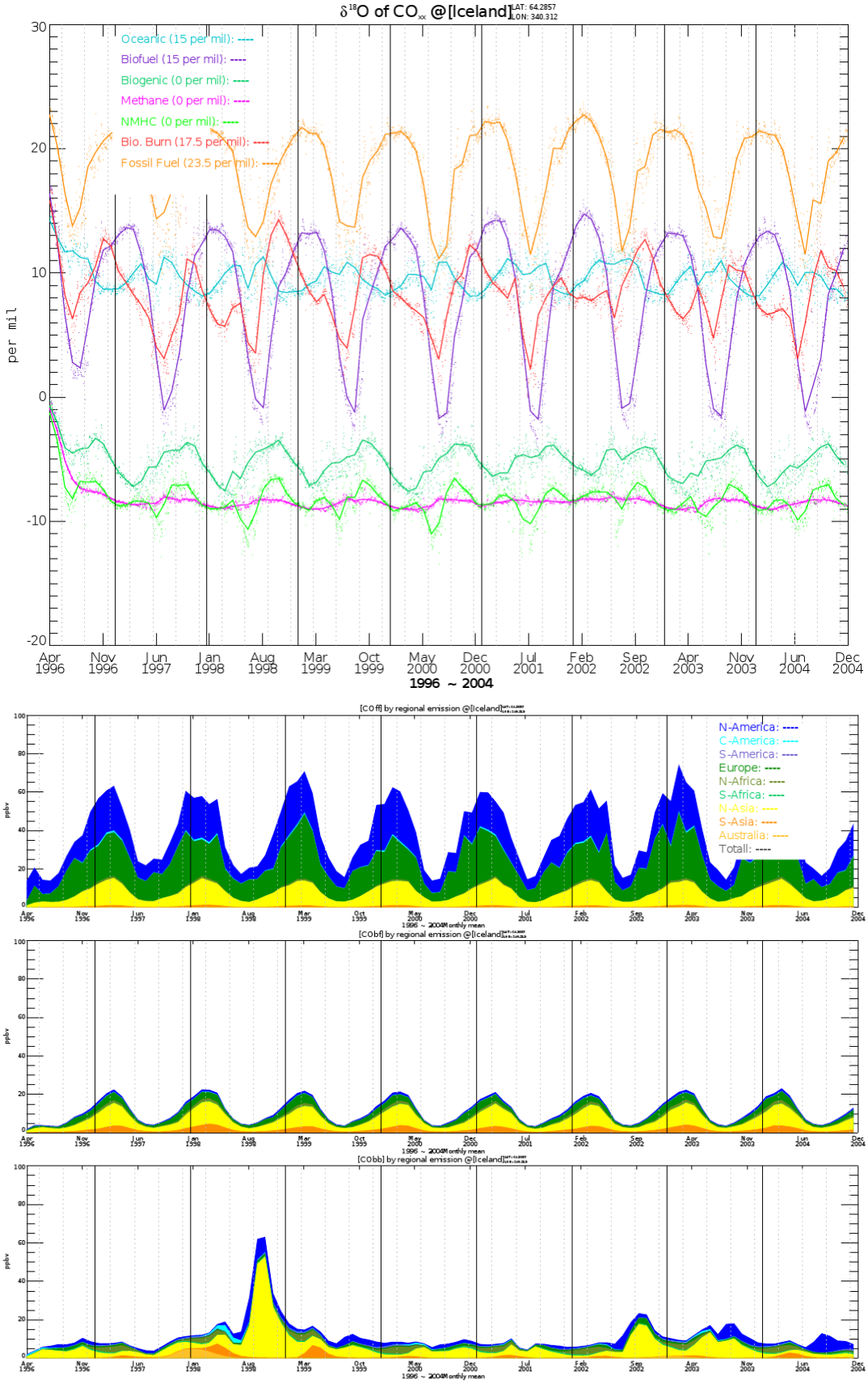

Figure S3. *Cont.*

Izana

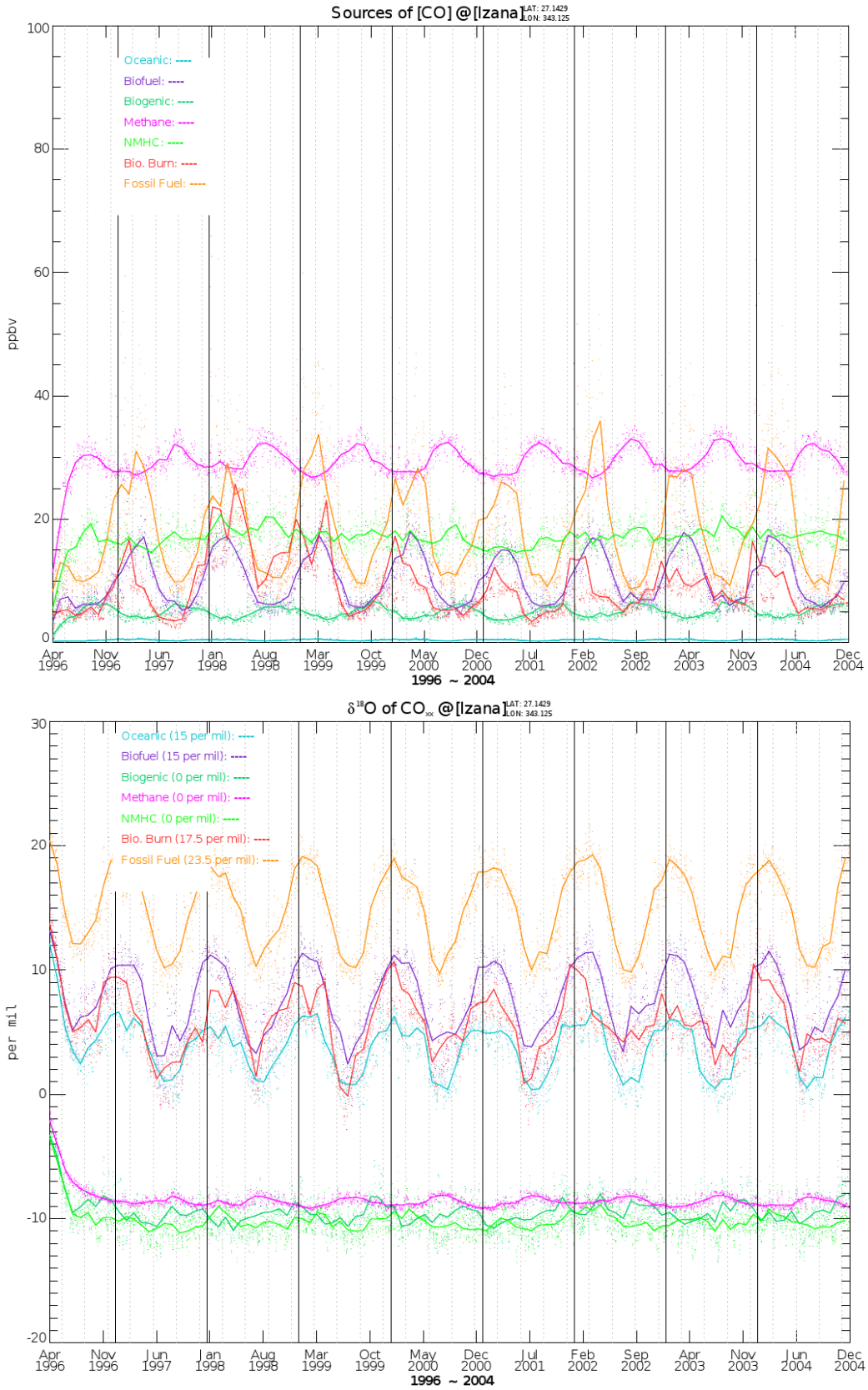

Figure S3. *Cont.*

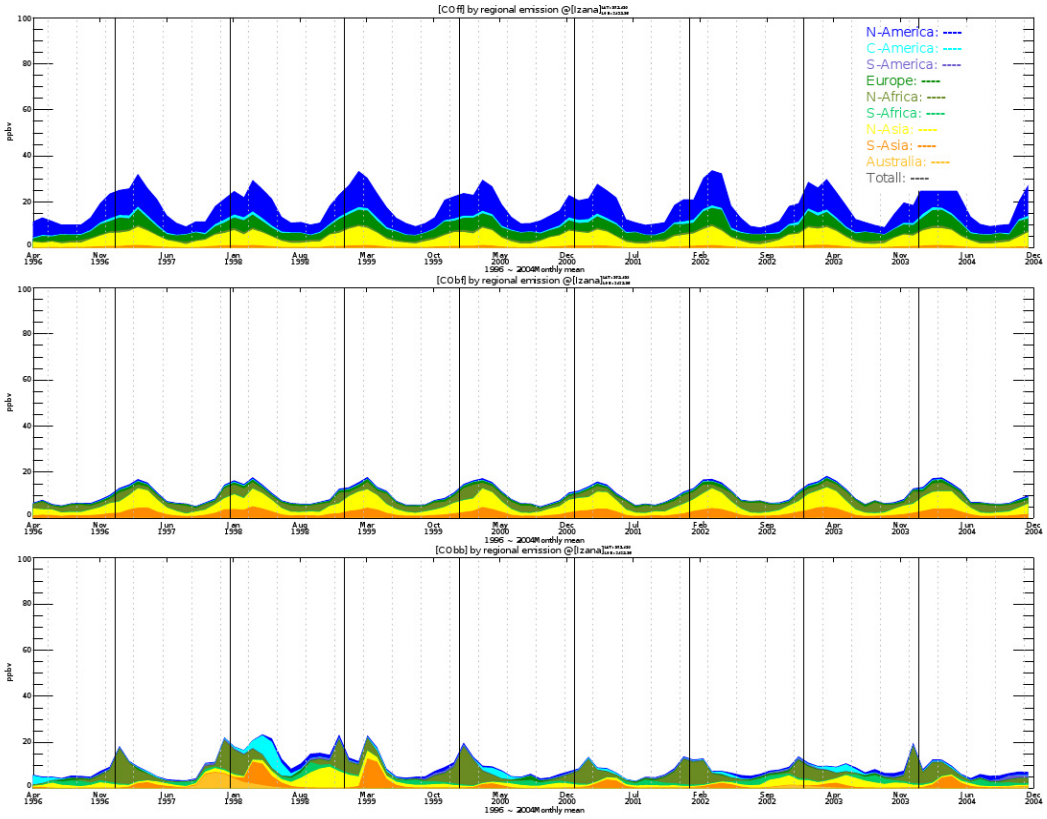

Mauna Loa

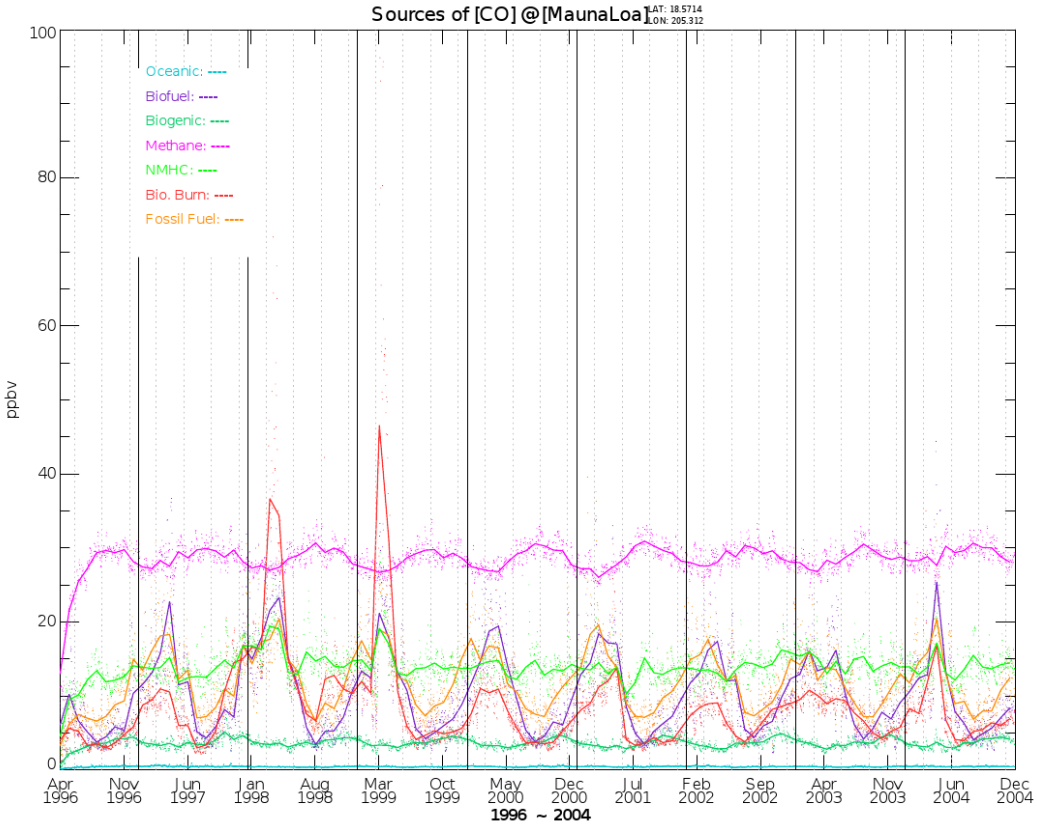

Figure S3. *Cont.*

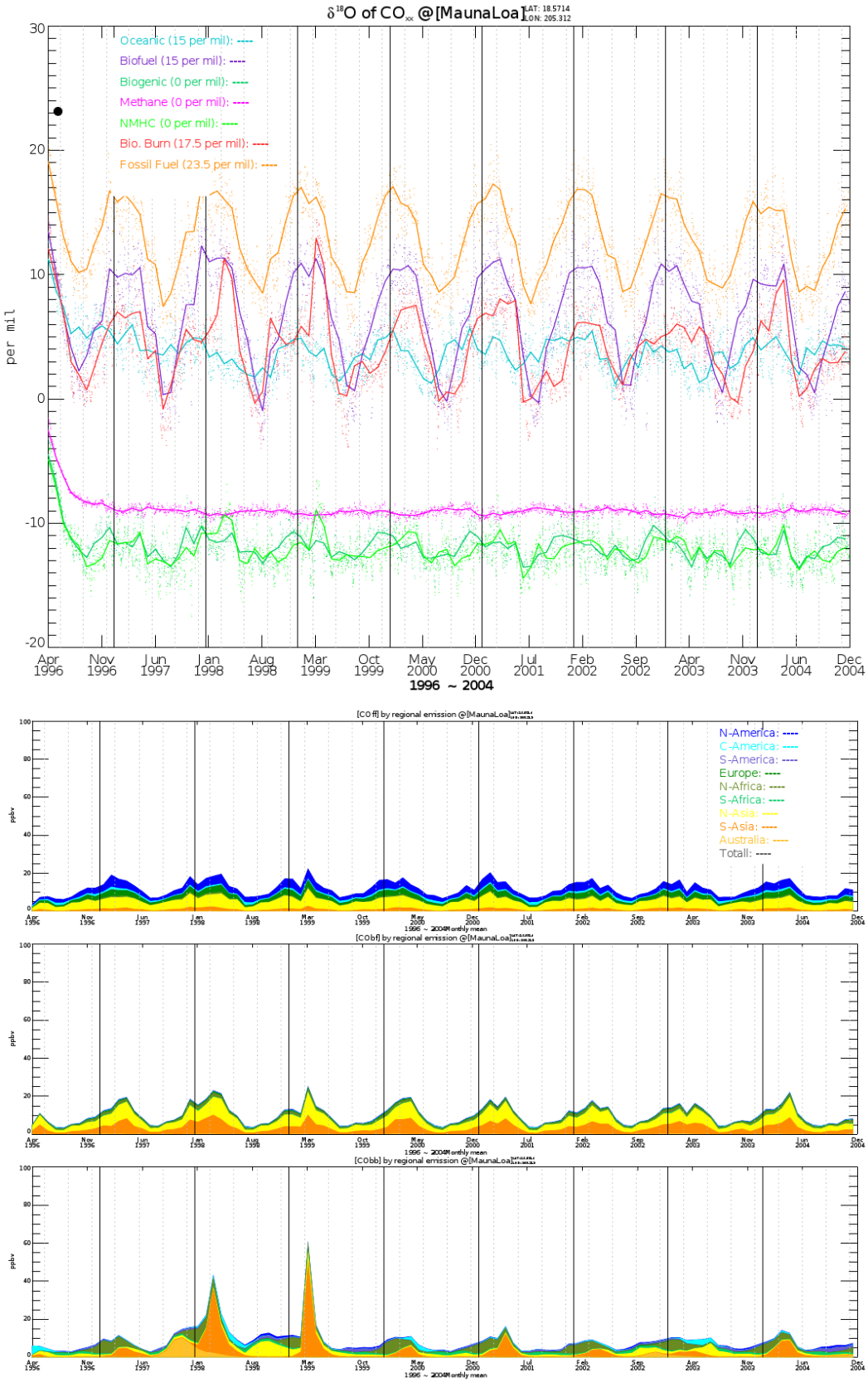

Figure S3. *Cont.*

Barbados

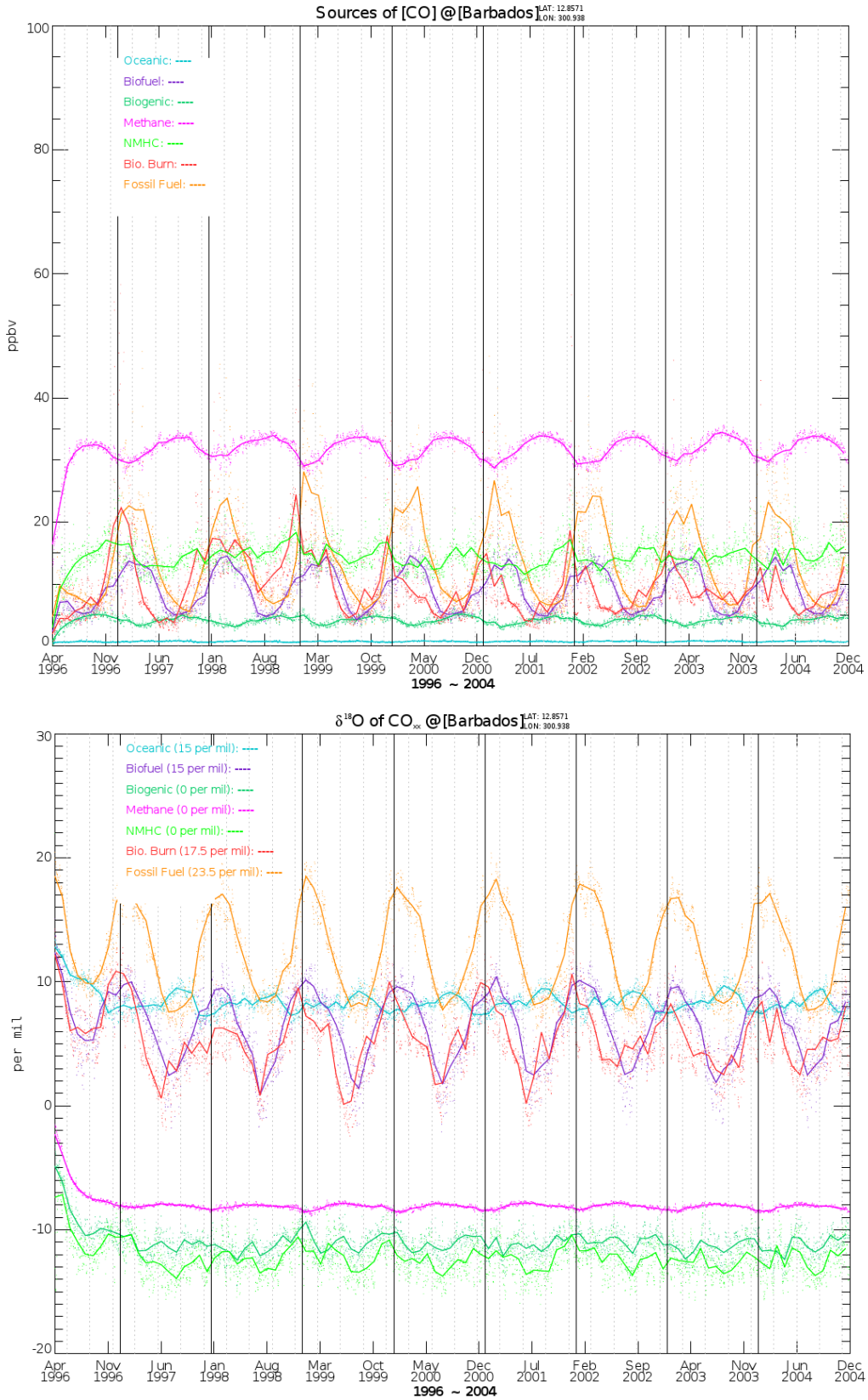

Figure S3. *Cont.*

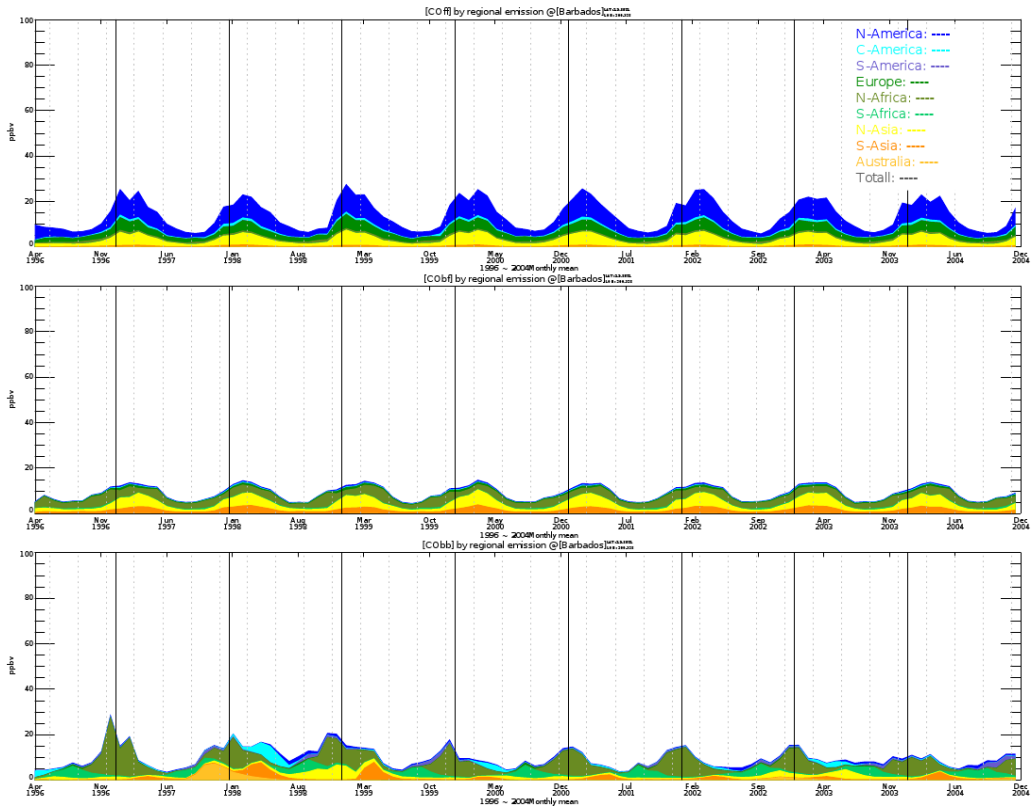

Baring head

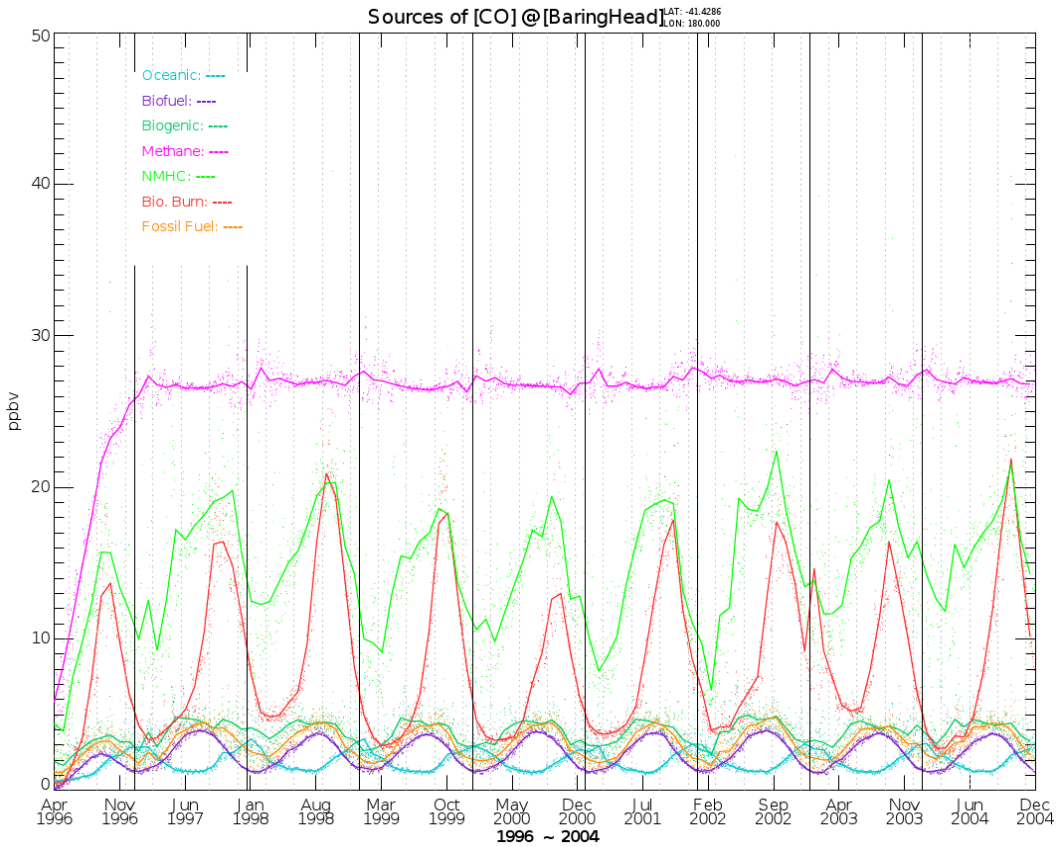

Figure S3. *Cont.*

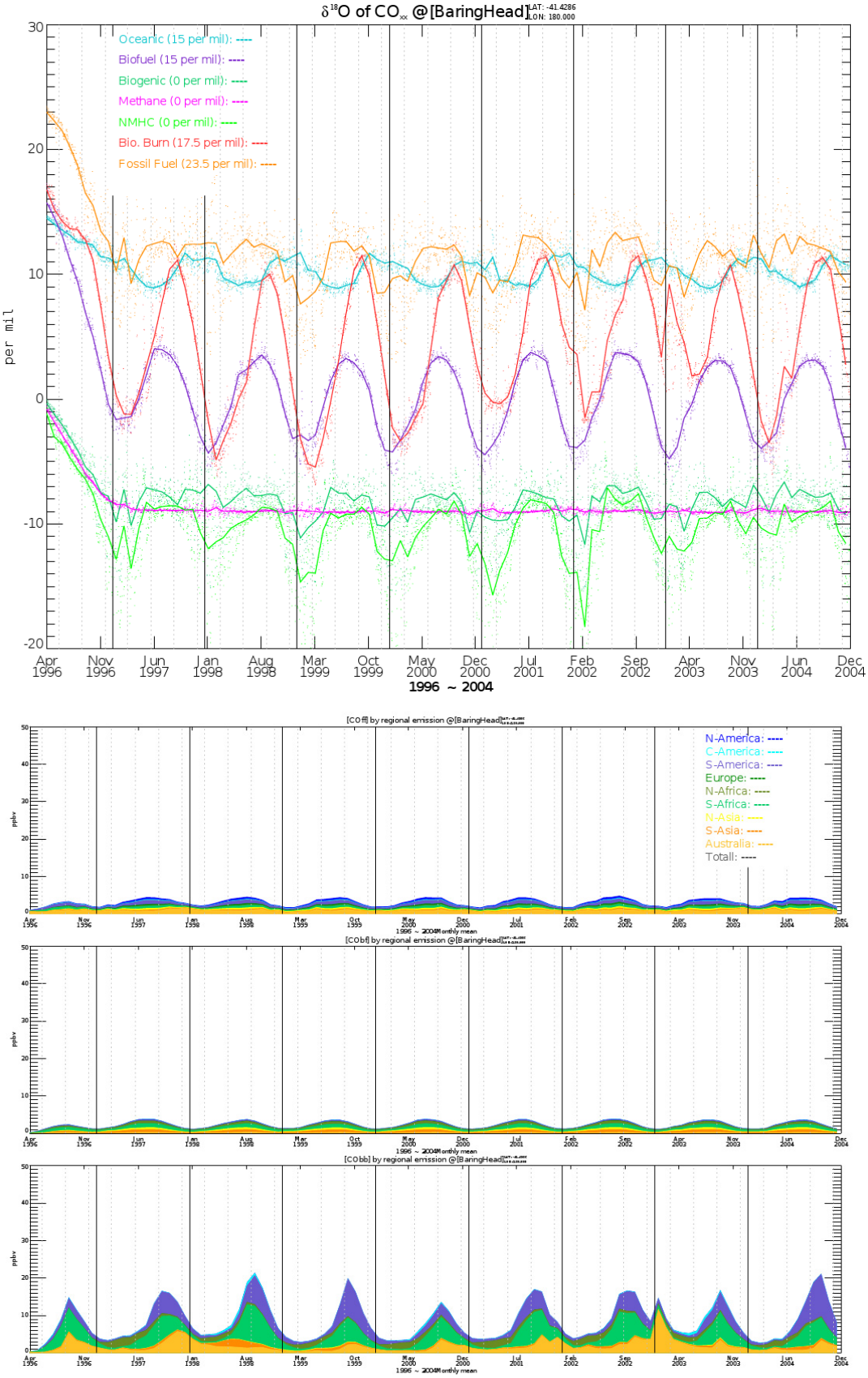

Figure S3. *Cont.*

Scott Base

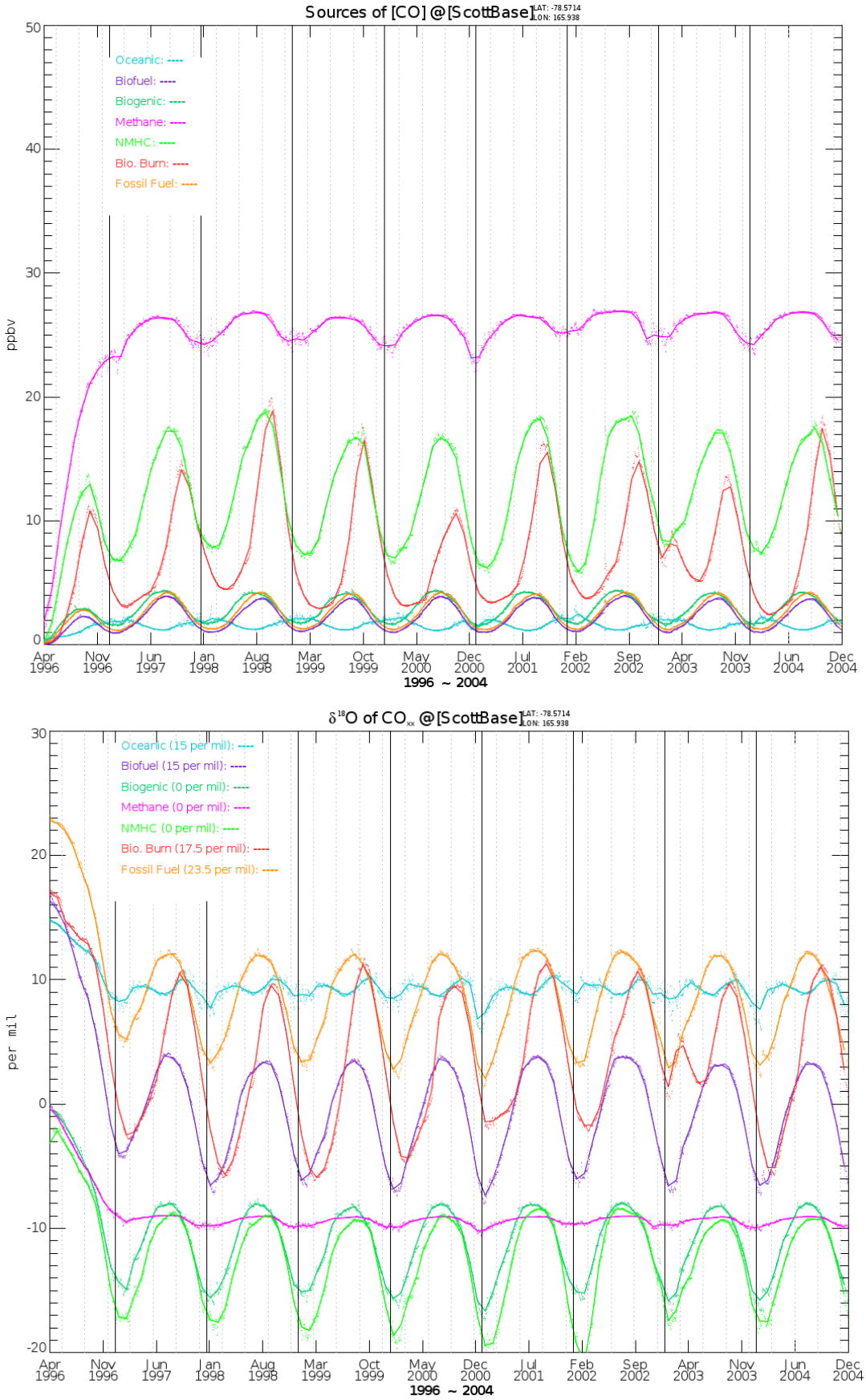

Figure S3. *Cont.*

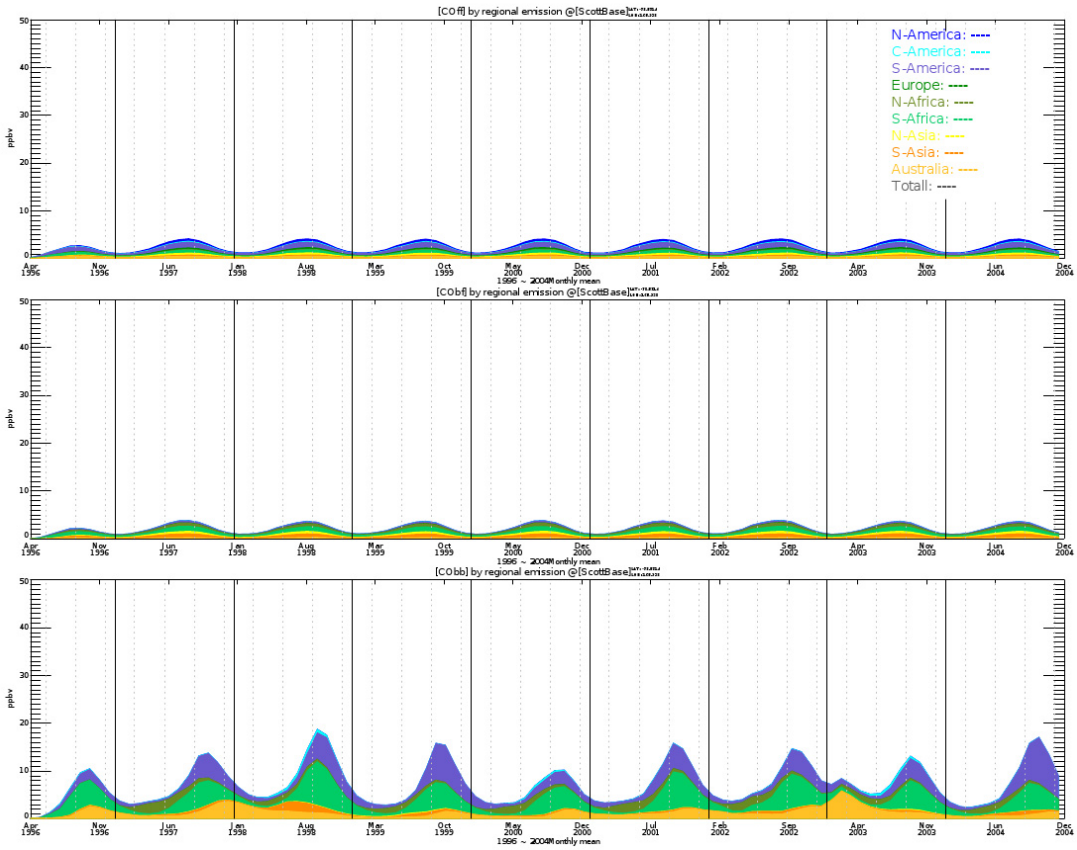

Figure S3. MOZART-4 simulation results: contribution (concentration) of CO sources at each station (the first panel of each station), time series of $\delta^{18}O$ by each source at each station (the second panel of each station) and contribution of CO sources for each geographic emission region (FF, BF and BB only). For the time series of $\delta^{18}O$, the isotopic source signature of each source are shown in the legend.

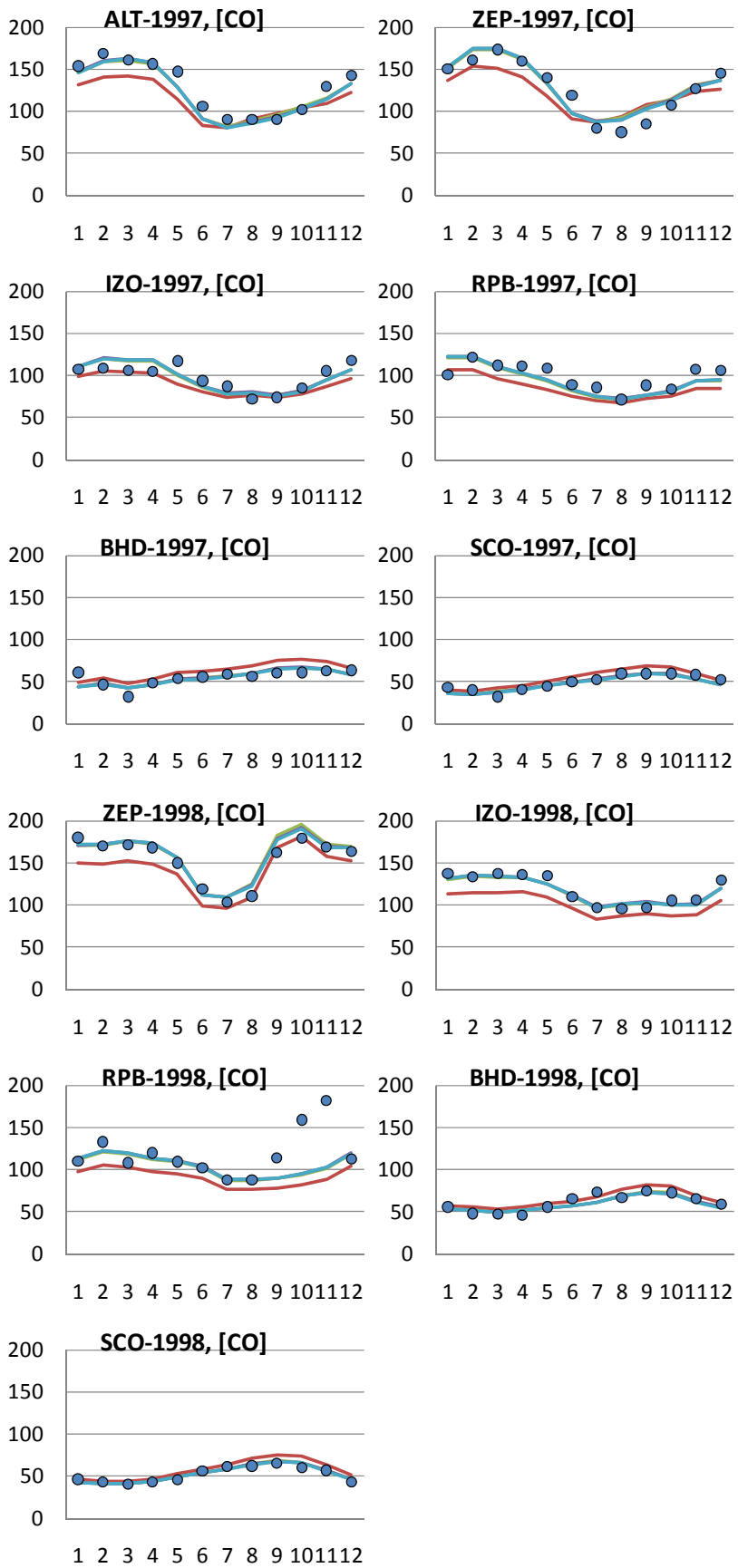

Figure S4. *Cont.*

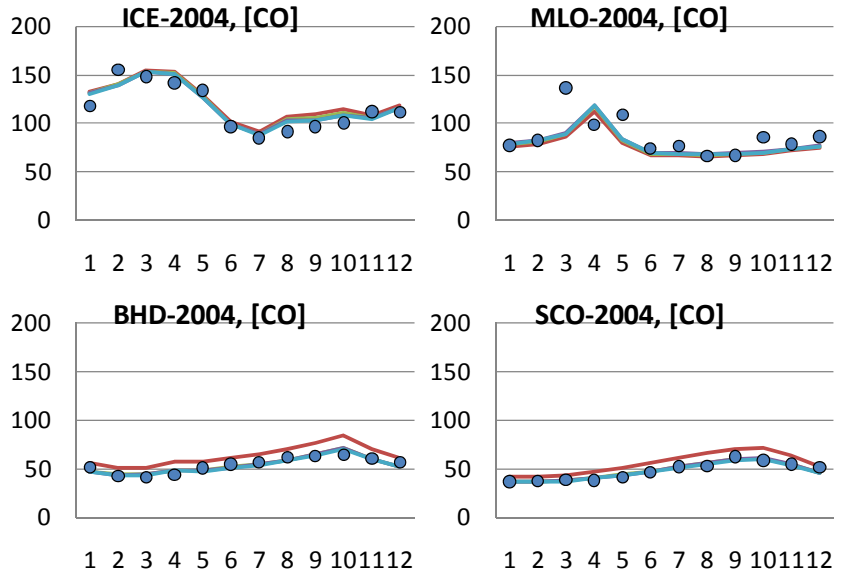

Figure S4. Comparison of *a priori* (brown line) and *a posteriori* (blue line) modeled surface [CO] with measurements (blue dots).

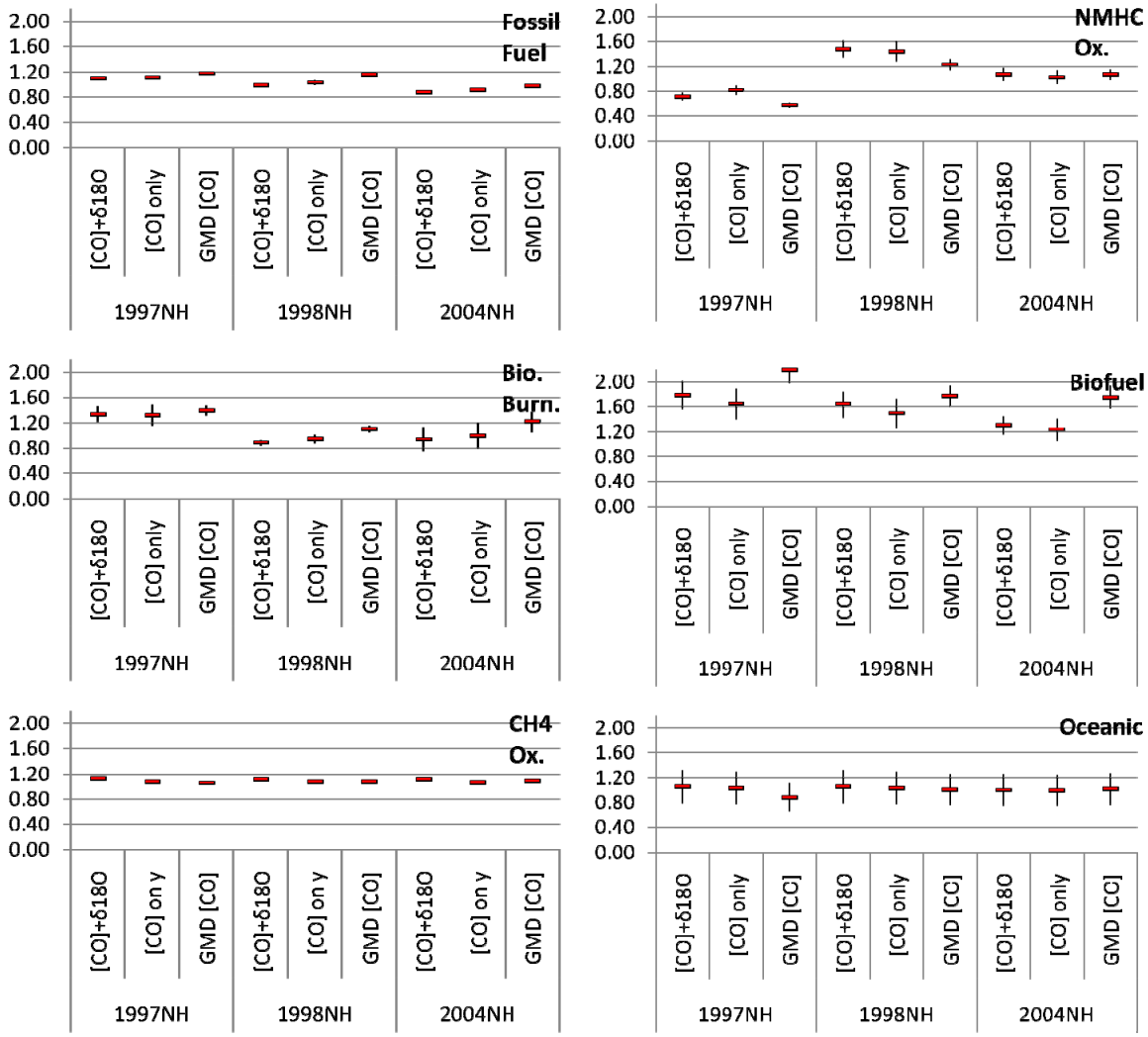

Figure S5. *Cont.*

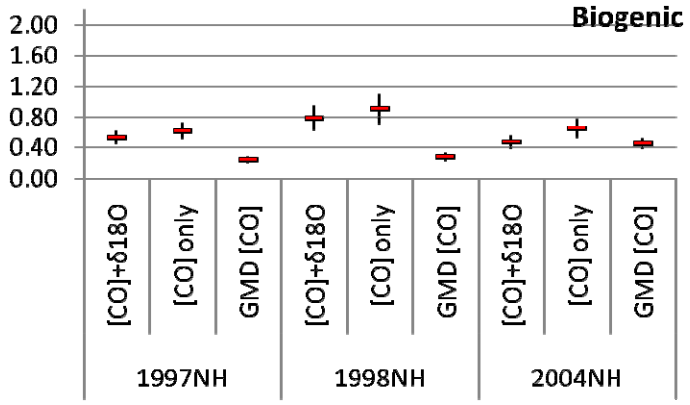

Figure S5. Comparison of optimization factors calculated from joint simultaneous inversion ([CO]+δ^{18}O), [CO]-only inversion and [CO]-only inversion using NOAA GMD [CO] (GMD[CO]). To get the [CO]NOAA inversion results, the following 11 NOAA GMD sampling sites are selected: Christmas Island, Republic of Kribati (lat 1.7°, lon −157.17°), Mariana Island, Guam (lat 13.43°, lon 144.78°), Cape Kumukahi, Hawaii, United States (lat 19.52°, lon −154.82°), Assekrem, Algeria (lat 23.18°, lon 5.42°), Key Biscayne, Florida, United States (lat 25.67°, lon −80.20°), Sede Boker, Negev Desert, Israel (lat 31.13°, lon 34.88°), Terceira Island, Azores, Portugal (lat 38.7°, lon −27.38°), Ulaan Uul, Mongolia (lat 44.45°, lon 111.10°), Park Falls, Wisconsin, United States (lat 45.93°, lon −90.27°), Baltic Sea, Poland (lat 55.35°, lon 17.22°), Barrow, Alaska, United States (lat 71.32°, lon −156.60°).